Supporting Information

McCartney et al. 10.1073/pnas.1411117111

SI Materials and Methods

All experiments with animals were performed in compliance with guidelines of the University Committee on Use and Care of Animals of the University of Michigan and the NIH.

Cell Culture. For dissociated postnatal day 1 (P1)–P2 rat and WT mouse (C57BL/6) hippocampal cultures for electrophysiology and immunofluorescence, cells were plated at a density of 230–460 cells per square millimeter in poly-D-lysine–coated, glass-bottomed Petri dishes (Mattek) as previously described by Sutton et al. (1) and maintained for at least 21–24 days in vitro (DIV) at 37 °C in growth medium [Neurobasal A (10888022; Invitrogen) supplemented with B27 (17504044; Invitrogen) and Glutamax (35050061; Invitrogen)] before use. For inositol labeling and measurement of phosphoinositides, rat hippocampal neurons were plated on 35-mm dishes. For WT and $Vac14^{-/-}$ experiments, embryonic day 18 embryos from crosses of $Vac14^{+/-}$ heterozygous mice (C57BL/6) were genotyped and dissociated hippocampal cultures were prepared similarly, except the culture medium was Neurobasal (21103049; Invitrogen).

Electrophysiology. Whole-cell patch-clamp recordings of mEPSCs were made with an Axopatch 200B amplifier from cultured hippocampal neurons bathed in Hepes-buffered saline [HBS; 119 mM NaCl, 5 mM KCl, 2 mM $CaCl_2$, 2 mM $MgCl_2$, 30 mM glucose, 10 mM Hepes (pH 7.4)] plus 1 μM TTX and 10 μM bicuculline. The pipette internal solution contained 100 mM cesium gluconate, 0.2 mM EGTA, 5 mM $MgCl_2$, 40 mM Hepes, 2 mM Mg-ATP, 0.3 mM Li-GTP, and 1 mM QX314 (pH 7.2), and had a resistance of 3–5 MΩ. mEPSCs were analyzed offline using MiniAnalysis (Synaptosoft) and custom MATLAB (MathWorks) scripts.

Lentivirus shRNA Knockdown of Mouse PIKfyve. For knockdown of mouse PIKfyve, MISSION shRNA lentiviral plasmid pLKO.1-puro with shRNA CCGGGCCAGTCGTAACATATTCTTACTCGAGTAAGAATATGTTACGACTGGCTTTTT (catalog no. TRCN0000025096 and clone ID NM_011086.1-949s1c1; Sigma–Aldrich) containing 811–831 nt of mouse PIKfyve cDNA (underlined) was used as described by Zolov et al. (2) at a multiplicity of infection (MOI) of 5, without polybrene. As a control, MISSION nontarget shRNA lentiviral control vector SHC002 with nonhuman or mouse shRNA was used at a MOI of 5. Neurons were incubated with virus for 1 h, and virus-containing medium was replaced with saved conditioned medium. Experiments were performed after 1 wk of lentivirus transduction.

Elevation of $PI(3,5)P_2$ Levels with $PIKfyve^{KYA}$ Mutation. Flp-In T-Rex 293 cells (R780-07; Life Technologies) were transfected with pcDNA5-FRT vectors that carry 3× FLAG, 3× FLAG-Citrine-PIKfyve (human), or 3× FLAG-Citrine-$PIKfyve^{KYA}$. Stable clones were selected according to the manual. Stably transfected cells were maintained in DMEM supplemented with 10% FBS, 1× penicillin/streptomycin/glutamate (Pen/Strep/Glutamate; 10378; Life Technologies), 15 μg/mL Blasticidin S HCl (A11139; Life Technologies) and 0.4 mg/mL Hygromycin B (10687; Life Technologies). For Western blots, cells were induced with 100 ng/mL doxycycline (D9891; Sigma) for 8 or 24 h and then harvested in radioimmunoprecipitation assay buffer [50 mM Tris (pH 7.4), 150 mM NaCl, 1 mM EDTA, 1% deoxycholic acid, 1% Nonidet P-40, 0.1% SDS, 10 mM NaF, 1 mM Na_3VO_4, 1× protease inhibitor mixture (04693116001; Roche)]. Antibodies used were mouse anti-FLAG (1:1,000, F3165; Sigma), rabbit anti-hFab1 (1:1,000, raised in-house) (3), and mouse anti-GAPDH (1:50,000, AM4300; Ambion). For lipid determination, cells were labeled as described for fibroblasts (see below), except that 100 ng/mL doxycycline was added 24 h before the extraction.

The sequences of the final clones used to make the Flp-In cell lines were verified as follows. Genomic DNA was prepared from Flp-In cell lines using the Qiagen DNeasy Blood and Tissue Kit. Citrine-PIKfyve and Citrine-$PIKfyve^{KYA}$ were PCR-amplified from genomic DNA using Thermo Scientific Phusion Polymerase. Full PCR coverage of the gene was obtained with five primer pairs:

Pair 1: Forward (Fwd), CGCAAATGGGCGGTAGGCGTG; Reverse (Rev), TAAAAGGGGGCTCATCTTGA

Pair 2: Fwd, CTGGTGAACCGCATCGAG; Rev, AGCCTCCTCTTAGCTTGATTG

Pair 3: Fwd, TGGTTGTCAATGGCTTTGTT; Rev, TCCTGCAACCTGTTATTCCA

Pair 4: Fwd, GCACCAGTATACTCGCAGAGC; Rev, TGTCCCATGTAAATGTTCG

Pair 5: Fwd, CGTCTGGAAGTCCAGTCCTT; Rev, GCTGGTTCTTTCCGCCTCAGAAG

The absence of point mutations was confirmed by Sanger sequencing of PCR products by the University of Michigan Sequencing Core. Full sequence coverage was achieved using the following sequencing primers:

Fwd1: CTGGTGAACCGCATCGAG

Fwd2: AATGATTTGCCTCGATCTCC

Fwd4: TCCTCAAATACTCCTCTTTCAACA

Fwd6: TTTGATTTCTGACACTGGAGGA

Fwd7: TGGTTGTCAATGGCTTTGTT

Fwd8: TGCAGATATTTCAGTTGCCT

Fwd9: AGGCTGTTGCCTCTGTGAAG

Fwd11: CACCAGAGACTTTGTGTGCTCT

Fwd12: GCACCAGTATACTCGCAGAGC

Fwd14: GGATCCACAGACAGCCAAGT

Fwd16: CGTCTGGAAGTCCAGTCCTT

Rev1: TGTGGCTGTTGTAGTTGTACTCC

Rev2: TAAAAGGGGGCTCATCTTGA

Rev3: TGTCTGCGCCTAAAGGTTGT

Rev8: AGCCTCCTCTTAGCTTGATTG

Rev13: TCCTGCAACCTGTTATTCCA

The PIKfyve clone used to make the Flp-In cell line 3× FLAG-Citrine-PIKfyve is 100% identical to the GenBank sequence AAR19397. The only mutations in the Flp-In cell line 3× FLAG-Citrine-$PIKfyve^{KYA}$ are E1620K, N1630Y, and S2068A.

Transfection. For experiments with Citrine-PIKfyve or Citrine-$PIKfyve^{KYA}$, neurons were transfected with 2 μg of Citrine-PIKfyve WT or Citrine-$PIKfyve^{KYA}$ plasmid DNA and 1 μg of

mCherry plasmid DNA with a modified CalPhos Transfection kit (Clontech) protocol. After incubation with DNA, cells were briefly incubated in a 10% CO_2 incubator and DNA-containing medium was discarded. Experiments were performed 1 wk after transfection. For pHluorin-GluA live endocytosis assay, neurons were transfected with 1 μg of SEP-GluA2(R607Q) (plasmid 24002; Addgene) or 1 μg of SEP-GluA1 (plasmid 24000; Addgene) and 1 μg of mCherry at DIV20. Experiments were performed 24–48 h later. For experiments with the fluorescent reporter of $PI(3,5)P_2$, neurons were transfected with 2 μg of mCherry-ML1N*2 plasmid DNA and 1 μg of EGFP plasmid DNA at DIV14 and treated with DMSO vehicle or 50 μM bicuculline the next day for 24 h. For experiments with HA-PIKfyve and EGFP or mCherry, neurons were transfected with 2 μg of HA-PIKfyve and 1 μg of EGFP or mCherry plasmid DNA 48 h before fixing and staining. For colocalization analysis of HA-PIKfyve with EGFP-LAMP1, neurons were transfected with 2 μg of HA-PIKfyve and 1 μg of EGFP-LAMP1 DNA 48 h before fixing and staining for HA, GFP, and MAP2.

Inositol Labeling and Measurement of PIPs. Mouse primary fibroblasts from C57BL/6 mice were cultured in DMEM (no. 11965; Life Technologies) supplemented with 15% FBS (no. 16000; Life Technologies) and 1× Pen/Strep/Glutamate. After reaching 60% confluence, fibroblasts were washed with PBS and custom-labeled in inositol-free DMEM (catalog no. 11965092; Life Technologies); 10 μCi/mL myo-[2-^{3}H] inositol (catalog no. NET1156005MC; PerkinElmer); 10% dialyzed FBS (no. 26400; Life Technologies); 20 mM Hepes, pH 7.2–7.5 (no. 15630; Life Technologies); 5 μg/mL transferrin (no. 0030124SA; Life Technologies); and 5 μg/mL insulin (no. 12585-014; Life Technologies) for 48 h. Toward the end of the labeling, cells were treated with 1 μM apilimod (Axon 1369; Axon Medchem BV) for 0 min, 2.5 min, 5 min, 30 min, and 120 min. Extraction and HPLC analysis are described in the study by Zolov et al. (2).

Primary rat hippocampal neurons were cultured for 21 d, rinsed with custom inositol-free Neurobasal-A (catalog no. ME120164L1; Life Technologies), and incubated for 24 h with inositol labeling medium containing inositol-free Neurobasal-A, 50 μCi/mL myo-[2-^{3}H] inositol, B27, and L-Glutamax (Invitrogen). Myo-[2-^{3}H] inositol-labeled cells were treated as described (2) with modifications. After 24 h, cultures were rinsed with HBS [119 mM NaCl, 5 mM KCl, 2 mM $CaCl_2$, 2 mM $MgCl_2$, 30 mM glucose, 10 mM Hepes (pH 7.4)] and treated 1 mL of 4.5% (vol/vol) perchloric acid for 15 min at room temperature. Cells were scraped off with a Cell Lifter (Costar 3008) and harvested at 12,000 × *g* for 10 min at 4 °C. Pellets were washed at room temperature with 1 mL of 0.1 M EDTA and resuspended in 50 μL of water. To deacylate lipids, samples were transferred to a glass vial, mixed with 1 mL of methanol/40% methylamine/L-butanol [45.7% methanol, 10.7% methylamine, 11.4% L-butanol (vol/vol)], and incubated at 55 °C for 1 h. Samples were vacuum-dried, resuspended in 0.5 mL of water, and extracted twice with an equal volume of butanol/ethyl ether/ethyl formate (20:4:1 vol/vol/vol). The aqueous phase was vacuum-dried and resuspended in 50 μL of water. Equivalent amounts of ^{3}H for each sample were analyzed by HPLC (Shimadzu UFLC CBM-20A Lite) using an anion exchange 4.6 × 250-mm column (no. 46211505; MAC MOD Analytical). A gradient of 1 M $(NH_4)_2HPO_4$, pH 3.8 (pH adjusted with phosphoric acid), was used at a flow rate of 1 mL/min, 0% for 5 min, 0–2% for 15 min, 2% for 80 min, 2–10% for 20 min, 10% for 65 min, 10–80% for 40 min, 80% for 20 min, and 80–0% for 5 min (all vol/vol). Radiolabeled eluate was detected with an inline flow scintillation analyzer (Beta-RAM model 5 RHPLC Detector; LabLogic). A 1:2 proportion of eluate to scintillant (Uniscint BD catalog no. LS-276-20L; National Diagnostics) was used with a flow rate of 3 mL/min. Fractions were analyzed by binning counts every 6 s. The data were collected and analyzed by Laura-4 software (LabLogic).

For comparison of PI polyphosphate levels, the raw counts in each peak were expressed as a percentage of total PI, calculated from summation of the counts of seven detectable peaks: PI, PI3P, PI4P, PI5P, $PI(3,5)P_2$, $PI(4,5)P_2$, and $PI(3,4,5)P_3$. $PI(3,4)P_2$ was not always detected. Background was calculated from adjacent regions and subtracted from all peaks. For standards, except for $PI(3,4,5)P_3$ and $PI(3,4)P_2$, extracts from yeast treated with 0.9 M NaCl for 5 min (4) were used. For $PI(3,4,5)P_3$ and $PI(3,4)P_2$ standards, radioactive products of PI3K phosphorylation of the phosphoinositide substrates $PI(4,5)P_2$ or PI4P, respectively, using ^{32}P were extracted, separated using TLC, and analyzed by HPLC.

For analysis of the mCherry-ML1N*2 distribution in neurons, we measured the overall intensity in the dendrite normalized to the average soma intensity to control for the level of expression, and we calculated the ratio of signal in the dendrite to soma in control or bicuculline-treated neurons.

Immunocytochemistry. Primary antibodies used were GluA2 mouse mAb (MAB397; Millipore), PSD-95 rabbit polyclonal antibody (pAb) (AB18258; Abcam), EEA1 rabbit mAb (C45B10 3288; Cell Signaling), vGLUT1 guinea pig pAb (AB5905; Millipore), GFP chicken pAb (AB16901; Millipore), HA mouse mAb (Clone 16B12; Covance), and MAP2 rabbit pAb (AB5622; Millipore). Secondary antibodies were conjugated to Alexa Fluor 488, 555, and 647 (Life Technologies). To label surface GluA2 and PSD-95, neurons were incubated live with the sGluA2 antibody for 15 min at 37 °C, rinsed with HBS, fixed with 2% paraformaldehyde and 2% sucrose, blocked with 2% BSA in PBS with 1 mM $MgCl_2$ and 0.1 mM $CaCl_2$ (PBS-MC) for 16 min, and incubated with fluorescent secondary antibody (goat anti-mouse 488). Cells were then permeabilized with 0.2% Triton X-100 for 10 min and blocked before incubation with PSD-95 antibody and, later, goat anti–rabbit-555 antibody. To label both surface GluA2 and internal GluA2, neurons were fixed for 4 min with 4% paraformaldehyde/4% sucrose, blocked with 2% BSA for 20 min, and incubated with GluA2 antibody overnight. Cells were washed twice with PBS-MC, incubated with goat anti-mouse IgG2a-488 for 1 h, and fixed with 4% paraformaldehyde/4% sucrose for 12 min. Then, cultures were permeabilized, blocked, and incubated with GluA2 antibody and rinsed and incubated with goat and mouse IgG2a-555. In all of the other experiments, neurons were fixed with 4% paraformaldehyde/4% sucrose in PBS-MC for 16 min, permeabilized with 0.2% Triton X-100 for 10 min, blocked with 2% BSA for at least 20 min, and incubated with primary antibody overnight. Images were acquired with an Olympus FV1000 confocal microscope (z-series, 0.41- to 0.45-μm intervals) and analyzed with Fiji (ImageJ; NIH) (5), Excel (Microsoft), and MATLAB (MathWorks).

Fluorescent Recovery After NMDA Stimulation. At DIV21, neurons transfected with either pHluorin-GluA2(Q) or pHluorin-GluA1 plasmids were rinsed with warm extracellular imaging buffer [25 mM Hepes, 120 mM NaCl, 5 mM KCl, 1 mM $CaCl_2$, 2 mM $MgCl_2$, 30 mM D-glucose, 1 mM TTX (pH 7.4)] to remove the media and then continuously perfused with warmed imaging buffer on the confocal stage. Pyramidal-like transfected neurons were analyzed. Images were acquired once per minute for (*i*) 12 min at baseline, (*ii*) 5 min in 0.2 mM Mg^{2+} solution, (*iii*) 5 min in NMDA stimulation buffer [25 mM Hepes, 120 mM NaCl, 5 mM KCl, 1 mM $CaCl_2$, 0.2 mM $MgCl_2$, 30 mM D-glucose, 1 mM TTX, 20 mM NMDA, 10 mM glycine (pH 7.4)], and (*iv*) NMDA washout and recovery for 50 min in imaging buffer. The pHluorin and mCherry fluorescence was imaged with 488-nm and 559-nm excitation, respectively, through an oil objective with a magnification of 60×.

Image Quantification. For all images, analysis was performed on images that were maximally Z-projected in Fiji (ImageJ) (5). Quantification of surface GluA2 levels was analyzed by finding the average pixel intensity of the thickest primary dendrite of pyramidal-like neurons at user-defined thresholds. Experimental groups were normalized to the average control intensity. For the time course analysis of changes in surface GluA2 and internal GluA2 levels with NMDA stimulation, the soma average pixel intensity was measured for each channel and normalized to the baseline levels for each experiment group. The ratio of surface intensity to internal intensity was subsequently calculated by dividing the surface and internal intensities. For the analysis of HA-PIKfyve localization, confocal images were maximally Z-projected and the number of HA-PIKfyve, EEA1, or EGFP-LAMP1 puncta was determined manually.

Statistics. Statistical differences between experimental conditions were determined as indicated by *t* test, Kolmogorov–Smirnov test, one-way ANOVA, or Kruskal–Wallis ANOVA. Multiple comparisons were determined using the Tukey–Kramer post hoc test (MATLAB, MathWorks).

1. Sutton MA, et al. (2006) Miniature neurotransmission stabilizes synaptic function via tonic suppression of local dendritic protein synthesis. *Cell* 125(4):785–799.
2. Zolov SN, et al. (2012) In vivo, Pikfyve generates PI(3,5)P2, which serves as both a signaling lipid and the major precursor for PI5P. *Proc Natl Acad Sci USA* 109(43):17472–17477.
3. Zhang Y, et al. (2012) Modulation of synaptic function by VAC14, a protein that regulates the phosphoinositides PI(3,5)P_2 and PI(5)P. *EMBO J* 31(16):3442–3456.
4. Duex JE, Tang F, Weisman LS (2006) The Vac14p-Fig4p complex acts independently of Vac7p and couples PI3,5P2 synthesis and turnover. *J Cell Biol* 172(5):693–704.
5. Schindelin J, et al. (2012) Fiji: An open-source platform for biological-image analysis. *Nat Methods* 9(7):676–682.

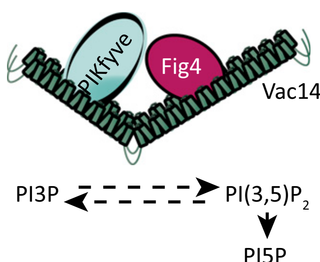

Fig. S1. Schematic of the PI(3,5)P_2 synthesis complex. The complex that regulates the synthesis of PI(3,5)P_2 is known to include PIKfyve, Fig4, and Vac14. PIKfyve, also known as Fab1, is the lipid 5-kinase that converts PI3P into PI(3,5)P_2. Fig4 is a lipid phosphatase and positive regulator of PIKfyve; therefore, loss of Fig4 leads to a reduction in PI(3,5)P_2 levels. Vac14 is primarily composed of Huntingtin, elongation factor 3, protein phosphatase 2A, and yeast kinase TOR1 (HEAT) repeats and functions as a scaffolding protein. There are likely other members of the complex that have not yet been identified.

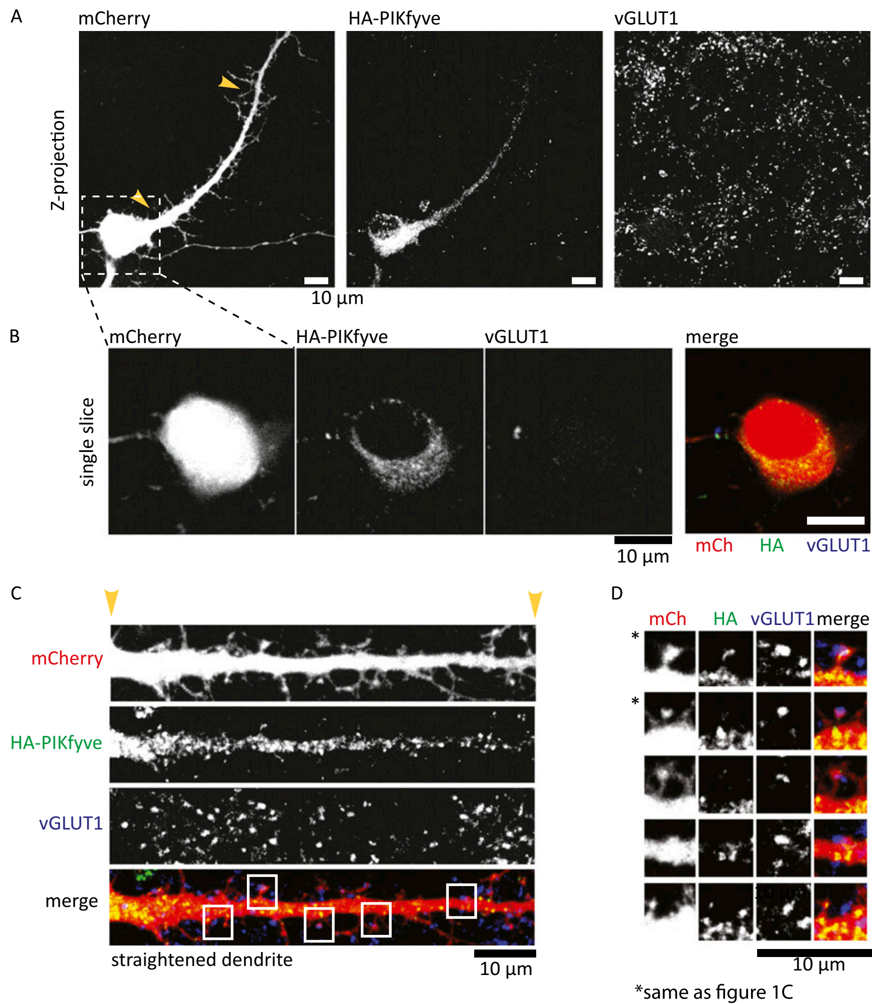

Fig. S2. PIKfyve is found at excitatory synapses. PIKfyve is distributed throughout neurons, including within dendritic spines, and is opposed to excitatory presynaptic terminals. Neurons were transfected with mCherry, a volume filler, and HA-PIKfyve. Confocal images were acquired following fixation and staining for HA and the presynaptic marker vGLUT1. (*A*) Representative Z-projected image of a transfected neuron expressing HA-PIKfyve and mCherry. The white dashed box indicates the region enlarged in *B*. Yellow arrowheads indicate the straightened dendrite in *C*. (*B*) Single slice through the neuron shows HA-PIKfyve puncta throughout the soma and an example of a bright HA-PIKfyve punctum with the presynaptic terminal opposed. mCh, mCherry. (*C*) Straightened dendrite with HA-PIKfyve puncta in dendritic spines and throughout the shaft. The white boxes indicate the spines presented and enlarged in *D*. For quantification, a putative synapse is defined as a vGLUT1 punctum that overlaps mCherry. There were 6.36 ± 0.35 total synapses per 10-µm dendrite and 2.66 ± 0.29 synapses with HA-PIKfyve per 10-µm dendrite (n = 30). (*D*) Examples of spines with or without HA-PIKfyve. *Same images as presented in Fig. 1*C*.

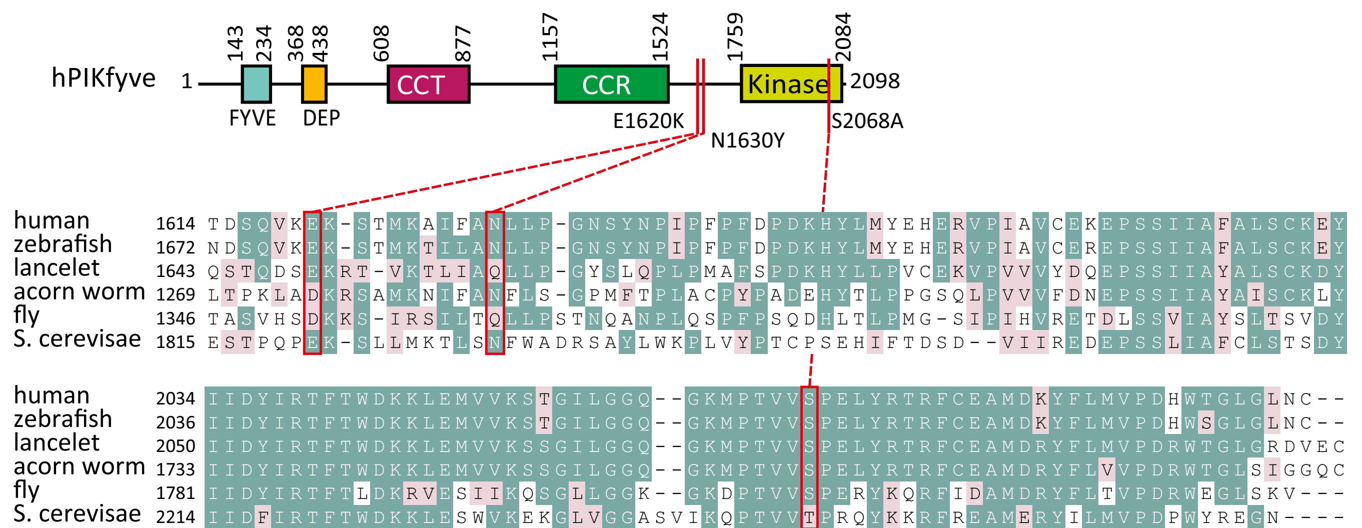

Fig. S3. Multiple alignments of PIKfyve homologs show high conservation. Domain structure of human PIKfyve. The domains shown are the following: FYVE (binds PI3P), DEP (dishevelled, Egl-10 and pleckstrin domain; function unknown), CCT (homologous to the chaperone Cpn60/TCP-1 family), CCR (conserved cysteine-rich domain), and kinase [catalytic site for conversion of PI3P to PI(3,5)P_2]. Multiple alignment of human (*Homo sapiens*, AAR19397.1), fish (*Danio rerio*, NP_001120777.1), lancelet (*Branchiostoma floridae*, XP_002598618.1), acorn worm (*Saccoglossus kowalevskii*, XP_006821423.1), fly (*Drosophila pseudoobscura*, XP_001361784), and yeast (*Saccharomyces cerevisiae*, BAA09258.1). PIKfyve homologs with conserved amino acids are shaded in teal, and conservative substitutions are shaded in pink. Red boxes indicate the mutated amino acids (E1620K, N1620K, and S2068A) in the PIKfyve^{KYA} mutant.

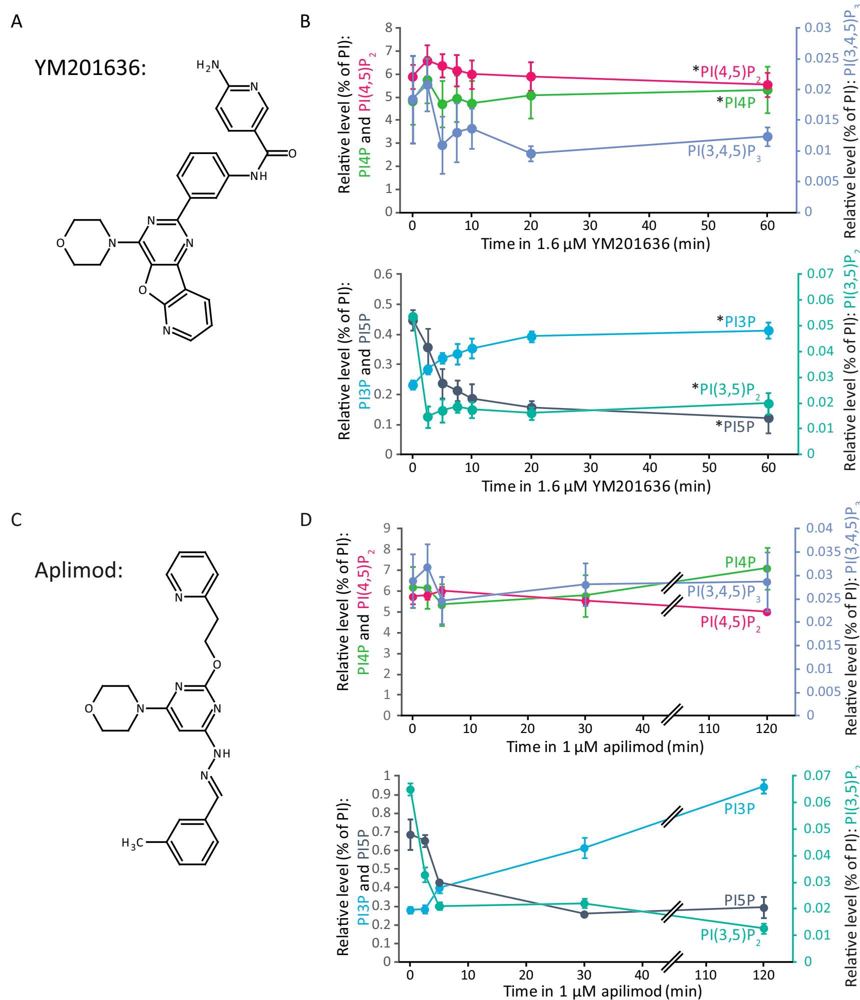

Fig. S4. PIKfyve inhibition rapidly depletes $PI(3,5)P_2$. (*A*) Chemical structure of YM201636. (*B*) Mean (±SEM) PIP levels in mouse primary fibroblasts after incubation with 1.6 μM YM201636 for the times indicated (*n* = 5) [*published previously by Zolov et al. (2)]. Analysis of the peak corresponding to $PI(3,4,5)P_3$ shows the 1.6 μM YM201636 reduces $PI(3,4,5)P_3$ levels by ~50%. (*C*) Chemical structure of apilimod. (*D*) Mean (±SEM) PIP levels in mouse primary fibroblasts after incubation with 1 μM apilimod for the times indicated results in a rapid depletion of $PI(3,5)P_2$ and PI5P and accumulation of PI3P (*n* = 3). The level of $PI(3,4,5)P_3$ does not change with 1 μM apilimod treatment.

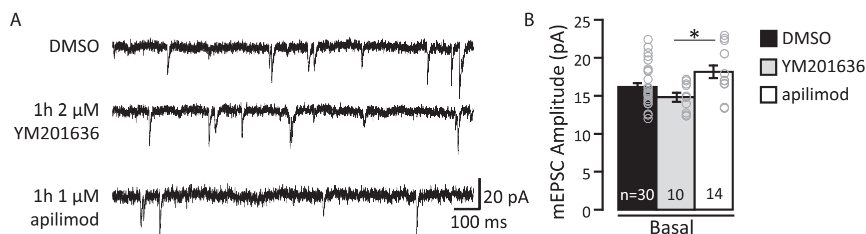

Fig. S5. PIKfyve inhibition alone does not drive strong changes in mEPSC amplitude. (*A*) Example electrophysiological recordings of mEPSCs in rat cultured hippocampal neurons (DIV21). The data for the DMSO group are the same data as depicted in Fig. 5*A*. (*B*) Mean (±SEM) mEPSC amplitude is similar following 1 h of PIKfyve inhibition with 1 μM apilimod or 1.6 μM YM201636. The dataset for the DMSO group is the same as the dataset that is presented in Fig. 5*B*. We found that in neurons with a history of normal neural activity, PIKfyve inhibition is not sufficient to increase mEPSC amplitude. Note that although neither inhibitor increased mEPSC amplitude above the mean amplitude of the DMSO control group, incubation with apilimod, but not YM201636, for 1 h increased mEPSC amplitude above the mean amplitude of the YM201636 group. This difference may be due to different off-target effects of each inhibitor. There is, however, a trend for increased amplitude in the apilimod group, suggesting that PIKfyve inhibition may predispose neurons to strengthening under some conditions [control + DMSO: 16.15 ± 0.49 pA, control + YM201636: 14.81 ± 0.60 pA, control + apilimod: 18.12 ± 0.84 pA; one-way ANOVA: $F(2,45) = 4.92$, $P = 0.0117$].*$P < 0.05$.

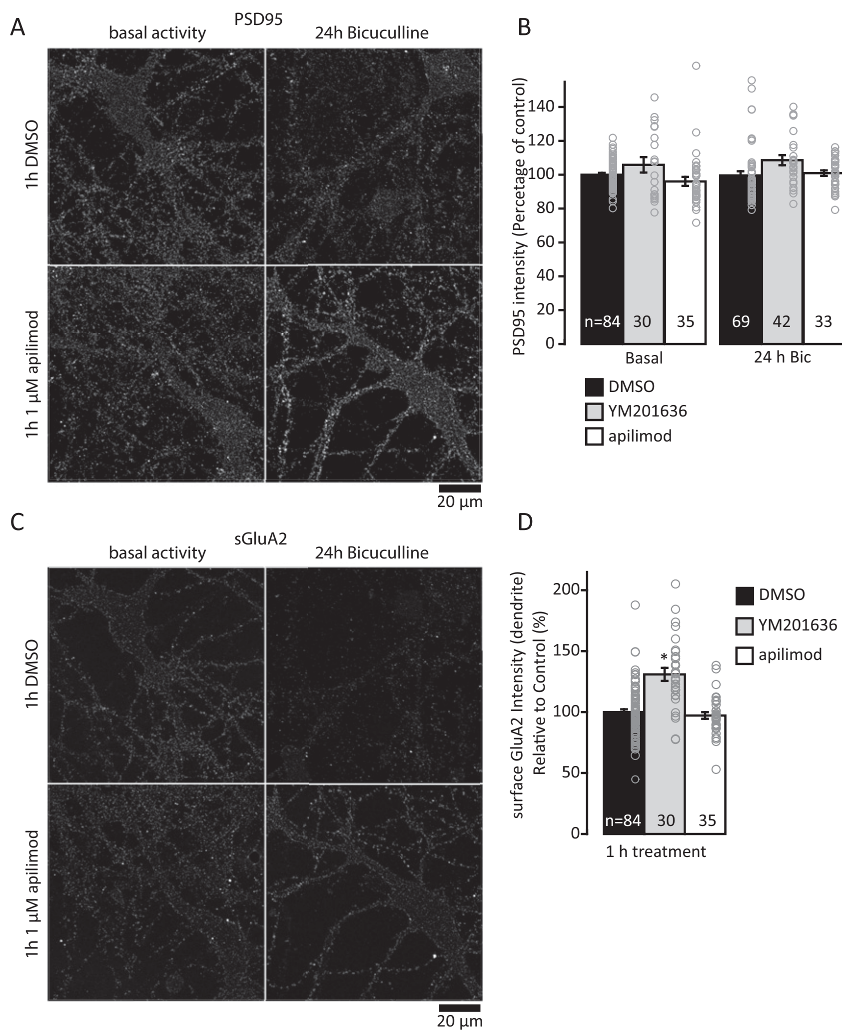

Fig. S6. PIKfyve inhibition after prolonged hyperactivation reverses the homeostatic decrease in surface GluA2. (*A*) Full-frame images of PSD-95 staining corresponding to the dendrites depicted in Fig. 5*C*. (*B*) Mean (±SEM) intensity of PSD-95 puncta. PSD-95 intensity is not affected by 50 μM bicuculline or by 1 h of PIKfyve inhibition with either 2 μM YM201636 or 1 μM apilimod. (*C*) Full-frame images of sGluA2 staining corresponding to the dendrites depicted in Fig. 5*E*. (*D*) Mean (±SEM) intensity of surface GluA2 puncta. Inhibition with 2 μM YM201636, but not 1 μM apilimod, for 1 h increased the surface levels of GluA2 [control: 100 ± 2.24%, 1 h of YM201636: 130 ± 93%, 1 h of apilimod: 95.49 ± 2.50%; one-way ANOVA: $F(2,145) = 26.12$, $P = 1.6e\text{-}10$]. *$P < 0.05$.

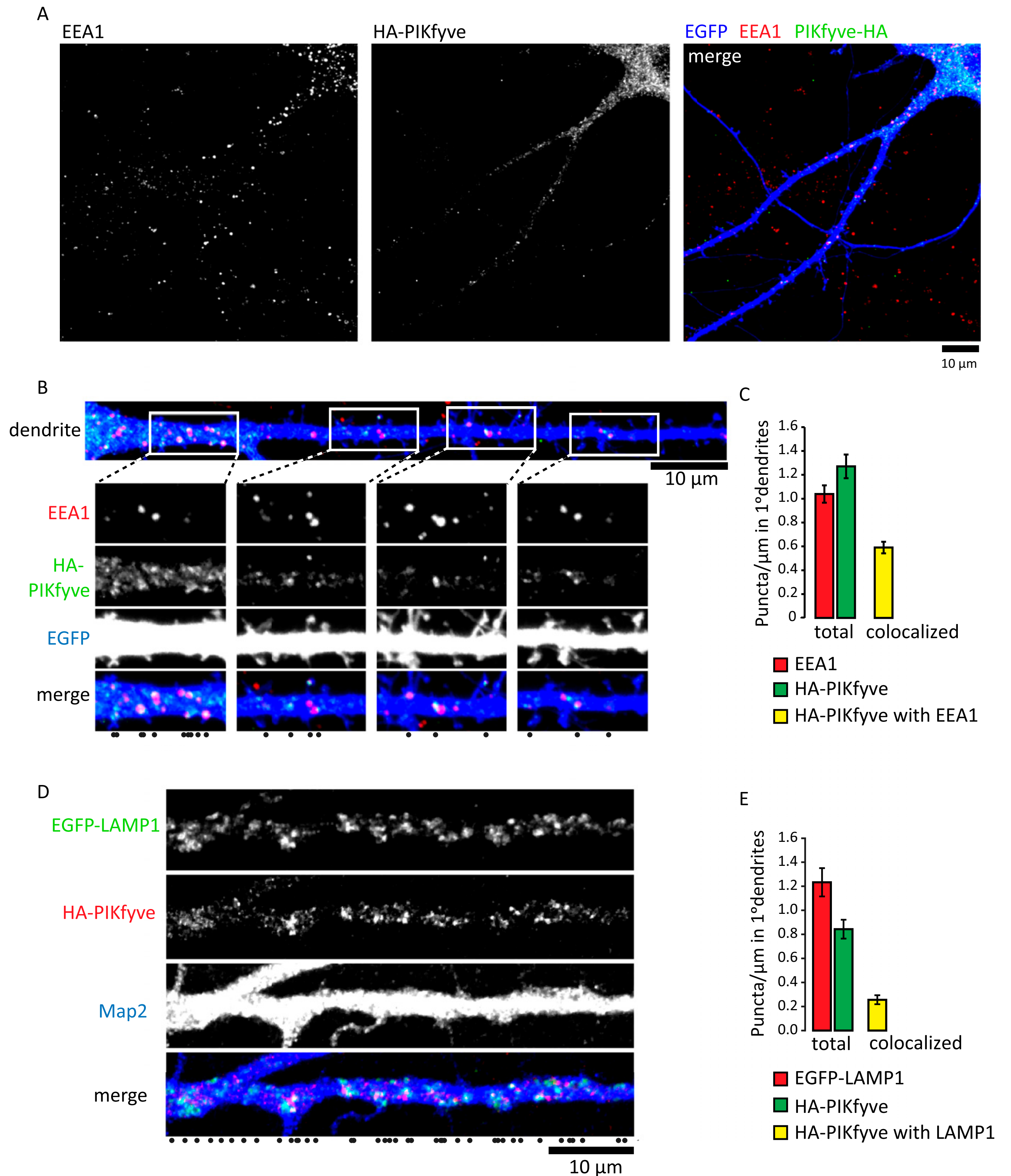

Fig. S7. PIKfyve is found on early endosomes and late endosomes/lysosomes. (*A*) Representative images of EEA1 staining (red) and a neuron transfected with GFP (note, shown in blue) and with HA-PIKfyve (green). HA-PIKfyve is found throughout the soma and dendrites. The merged image shows partial colocalization of HA-PIKfyve with EEA1 in the transfected neuron (triple overlap shown in white). (*B*) One dendrite in *A* was straightened and enlarged. White boxes indicate the regions of interest that are enlarged below. Many of the EEA1 puncta that overlap with the transfected neuron are also positive for HA-PIKfyve. Of particular relevance, multiple spines are positive for HA-PIKfyve and EEA1. There are also HA-PIKfyve puncta that do not overlap with EEA1. (*C*) Average (±SEM) puncta per micrometer in the first 55-µm dendrite. Total EEA1: 1.04 ± 0.07 puncta per micrometer. Total HA-PIKfyve: 1.27 ± 0.10 puncta per

Legend continued on following page

micrometer. HA-PIKfyve puncta that overlap with an EEA1 puncta: 0.59 ± 0.05 punctum per micrometer ($n = 48$ from three independent experiments). (*D*) Representative image of a dendrite with HA-PIKfyve (red), EGFP-LAMP1 (green), and MAP2 (blue) staining. The merged image shows partial colocalization of HA-PIKfyve with EGFP-LAMP1. (*E*) Average (±SEM) puncta per micrometer in the first 55-μm dendrite. Total eGFP-LAMP1: 1.23 ± 0.12 puncta per micrometer. Total HA-PIKfyve: 0.84 ± 0.08 punctum per micrometer. Total HA-PIKfyve puncta that overlap with LAMP1: 0.26 ± 0.04 punctum per micrometer ($n = 47$ from three independent experiments). Note that the HA-PIKfyve colocalization analysis with EEA1 or LAMP1 was performed in separate experiments with different preparations of cultured hippocampal neurons.

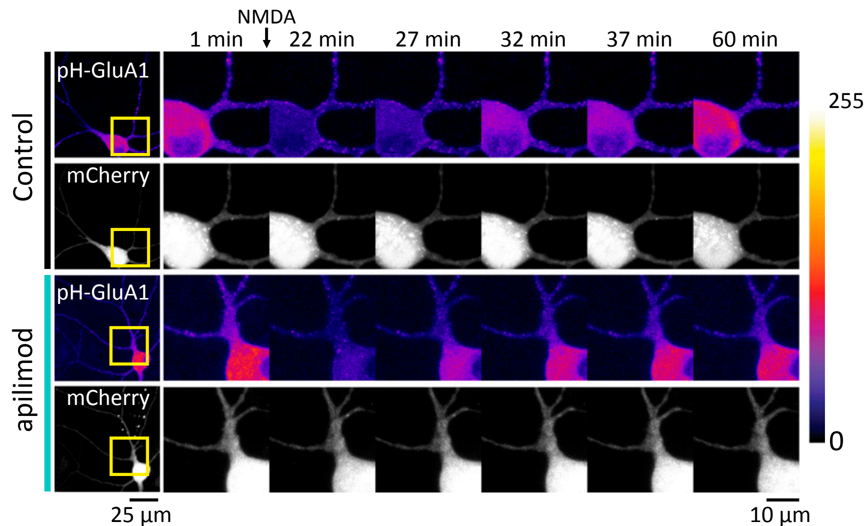

Fig. S8. Acute inhibition of PIKfyve does not have an impact on pHluorin-GluA1 trafficking. Representative images of neurons cotransfected with pH-GluA1 and mCherry. Neurons were incubated with DMSO or PIKfyve inhibitors for 1 h before live-confocal imaging. During imaging, all solutions were continuously perfused at 32 °C. Once a stable baseline was obtained, HBS (0.2 mM Mg^{2+}) was washed on for 5 min, followed by 5 min of stimulation with NMDA (20 μM NMDA, 10 μM glycine, 0.2 mM Mg^{2+}), which quenches the fluorescence of pH-GluA1. After NMDA stimulation, normal HBS was continuously perfused for the remainder of the experiment. The fluorescence of pH-GluA1 is strongly quenched by NMDA stimulation; however, brief PIKfyve inhibition does not have an impact on the rate of recovery.

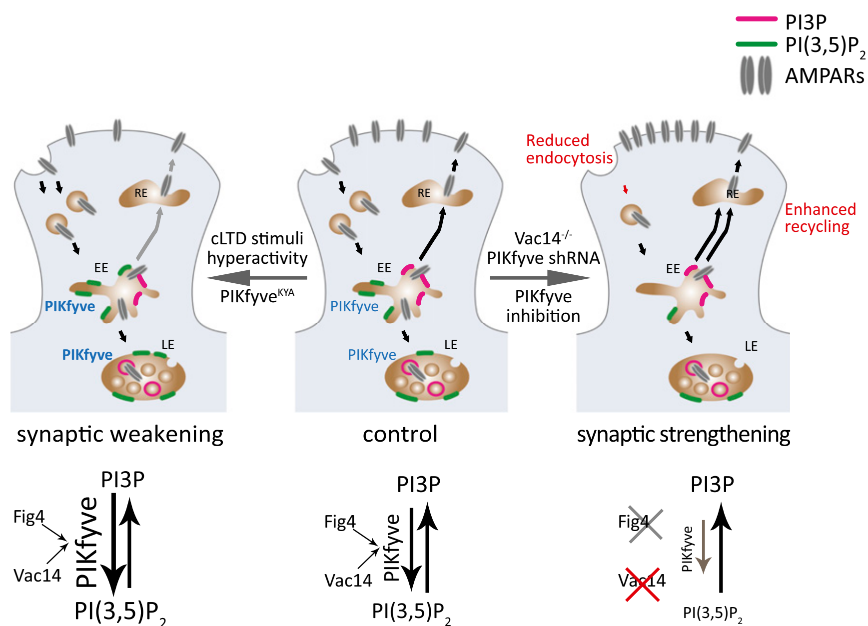

Fig. S9. Model for roles of PIKfyve in synaptic plasticity. PIKfyve is found at early endosomes (EEs) and late endosomes/lysosomes (LEs). Vac14, a regulator of PIKfyve, is also found at these locations (3). Together, these findings suggest that $PI(3,5)P_2$ (green) is generated at both EEs and LEs in proximity to synaptic sites on dendrites. (*Left*) In cultured hippocampal pyramidal neurons, synaptic weakening is associated with elevated $PI(3,5)P_2$ levels and decreased abundance of surface AMPARs. Elevation of $PI(3,5)P_2$ through the dominant active $PIKfyve^{KYA}$ mutant also results in synaptic weakening. These results suggest that PIKfyve activity plays critical roles in regulation of excitatory synapse strength. (*Right*) Lowered PIKfyve activity results in synaptic strengthening, enhancement of recycling, and reduction in endocytosis of AMPARs. Together, these findings suggest that PIKfyve function at EEs and LEs near synapses modulates AMPAR trafficking during activity-dependent changes in synapse strength.

Table S1. Comparison of PIP levels in mouse embryonic fibroblasts (MEFs) and cultured hippocampal rat neurons

	Percentage of PI (±SEM)	
PIP	MEF ($n = 5$)	Neuron ($n = 11$)
PI4P	3.276 ± 0.136	16.590 ± 1.274
$PI(4,5)P_2$	4.963 ± 0.251	13.188 ± 0.608
PI5P	0.306 ± 0.013	0.361 ± 0.027
PI3P	0.191 ± 0.011	0.206 ± 0.008
$PI(3,5)P_2$	0.042 ± 0.003	0.018 ± 0.002
$PI(3,4,5)P_3$	0.015 ± 0.002	0.023 ± 0.002

The mean PIP level under basal conditions for MEFs were reported previously in (2), except for $PI(3,4,5)P_3$. The mean PIP level for neurons was measured in cultured neurons metabolically labeled with myo-[2-^{3}H] inositol for 24 h. Immediately before cell precipitation with perchloric acid, the media were collected and cells were incubated in warm HBS for 5 min.